Extracellular histones are essential effectors of C5aR- and C5L2-mediated tissue damage and inflammation in acute lung injury

Markus Bosmann,[*,†] Jamison J. Grailer,[‡] Robert Ruemmler,[*,‡] Norman F. Russkamp,[‡] Firas S. Zetoune,[‡] J. Vidya Sarma,[‡] Theodore J. Standiford,[§] and Peter A. Ward[‡,1]

[*]Center of Thrombosis and Hemostasis and [†]Department of Hematology and Oncology, University Medical Center, Mainz, Germany; and [‡]Department of Pathology and [§]Department of Internal Medicine, Division of Pulmonary and Critical Care Medicine, University of Michigan Medical School, Ann Arbor, Michigan, USA

ABSTRACT   We investigated how complement activation promotes tissue injury and organ dysfunction during acute inflammation. Three models of acute lung injury (ALI) induced by LPS, IgG immune complexes, or C5a were used in C57BL/6 mice, all models requiring availability of both C5a receptors (C5aR and C5L2) for full development of ALI. Ligation of C5aR and C5L2 with C5a triggered the appearance of histones (H3 and H4) in bronchoalveolar lavage fluid (BALF). BALF from humans with ALI contained H4 histone. Histones were absent in control BALF from healthy volunteers. In mice with ALI, *in vivo* neutralization of H4 with IgG antibody reduced the intensity of ALI. Neutrophil depletion in mice with ALI markedly reduced H4 presence in BALF and was highly protective. The direct lung damaging effects of extracellular histones were demonstrated by airway administration of histones into mice and rats (Sprague-Dawley), which resulted in ALI that was C5a receptor-independent, and associated with intense inflammation, PMN accumulation, damage/destruction of alveolar epithelial cells, together with release into lung of cytokines/chemokines. High-resolution magnetic resonance imaging demonstrated lung damage, edema and consolidation in histone-injured lungs. These studies confirm the destructive C5a-dependent effects in lung linked to appearance of extracellular histones.—Bosmann, M., Grailer, J. J., Ruemmler, R., Russkamp, N. F., Zetoune, F. S., Sarma, J. V., Standiford, T. J., Ward, P. A. Extracellular histones are essential effectors of

THE ANNUAL INCIDENCE of acute lung injury (ALI) and acute respiratory distress syndrome (ARDS) approximates 200,000 cases in the United States, with mortality rates around 20–40% (1–4). There are currently no U.S. Food and Drug Administration (FDA)-approved pharmacologic therapies for ALI/ARDS (5). Acute lung injury (ALI) involves complement activation, as indicated by attenuated severity in C5-deficient mice following formation of immune-complexes (6, 7). Silencing of complement component C5a receptor 1 (C5aR; CD88) in lung epithelial cells reduces the severity of ALI (8). The pathology of ALI/ARDS is characterized by an acute inflammatory response associated with accumulation of polymorphonuclear neutrophils (PMNs), fibrin deposits, alveolar hemorrhage, and pulmonary edema fluid (5, 9, 10). Lung dysfunction is aggravated by injury of alveolar epithelial and vascular endothelial cells, leading to necrosis and apoptosis (5, 11). Inflammatory mediators such as IL-1α, IL-6, TNF-α, and leukotrienes, together with oxidants, proteases, and complement activation products, are thought to cause induction and progression of ALI/ARDS (5, 7, 12, 13). The complement system is structured as a cascade of >25 proteins serving innate immune defenses and homeostasis (14). Proteolytic cleavage of complement proteins generates the anaphylatoxins, complement components C3a, C4a, and C5a, the last displaying the highest inflammatory potency to induce inflammation (15, 16). C5a frequently requires

a costimulatory signal [*e.g.*, lipopolysaccharide (LPS) and N-formyl-Met-Leu-Phe] to trigger full biological effects, such as neutrophil activation and chemotaxis. In plasma, C5a is rapidly converted ($t_{1/2}$: <5 min) to biologically less active $C5a_{desArg}$ by carboxypeptidases (17). C5a may be more stable in extravascular compartments.

Both C5a and $C5a_{desArg}$ (with lower binding affinity) are ligands for CD88, a member of the G-protein-linked 7-transmembrane domain receptor family (18, 19). C5a interaction with C5aR initiates cytosolic Ca^{2+} increases and phosphorylation of MAP kinases in most cell types (7). Expression of C5aR is found in high numbers within the myeloid lineage, but T cells, as well as epithelial cells, endothelial cells and fibroblasts, also express C5aR in lower numbers (20–27).

C5a receptor 2 (C5L2; GPR77), shares 35% amino acid identity with C5aR and was initially described as a "default" receptor due to binding of both C5a and $C5a_{desArg}$ without traditional signaling properties (28, 29). However, controversy has arisen as to whether C5L2 was critically involved in proinflammatory functions of C5a (30, 31). For example, both C5aR and C5L2 modulate the inflammatory response during polymicrobial sepsis (32). C5L2 and C5aR play distinct roles in the C5a-dependent pathogenesis of experimental allergic asthma (33, 34). On the other hand, C5L2 is dispensable for regulation of many but not all macrophage-derived cytokines by C5a (20, 35–37). Overall, the sequence of events linking C5aR- and C5L2-mediated acute inflammation with ensuing lung damage and respiratory insufficiency is poorly understood.

The concept of neutrophil extracellular traps (NETs) has recently attracted considerable attention (38, 39). NETs are structures of extracellular histones and DNA that ensnare and kill bacteria (38). The formation of NETs is an orchestrated program involving activation of Raf/MEK/ERK signaling pathways (40), chromatin hypercitrullination (41), assembly of the multimeric NADPH oxidase complex, and generation of reactive oxygen species (ROS) (41, 42). NET formation in the circulation is promoted by platelet-leukocyte interactions and may subsequently trigger coagulation and thrombosis (43, 44). It remains unclear how complement activation affects the extracellular appearance of NET components such as histones.

In this report, we address the gap in knowledge of the molecular events by which C5a-induced inflammation progresses to tissue injury and loss of organ function. Our findings suggest a critical involvement for extracellular histones as mediators of acute pathology following ligation of C5a with C5aR and C5L2 in models of ALI.

MATERIALS AND METHODS

Animals

All procedures were performed in accordance with the U.S. National Institutes of Health guidelines and the University Committee on Use and Care of Animals (UCUCA), University of Michigan. Male mice of the strain C57BL/6J (10–16 wk) were from the Jackson Laboratories (Bar Harbor, ME, USA). $C5aR^{-/-}$ mice and $C5L2^{-/-}$ mice (45), backcrossed for >10 generations on C57BL/6J, were bred and genotyped at the University of Michigan. Sprague-Dawley rats (150–250 g) were from Charles Rivers Laboratories (Wilmington, DE, USA) or when implanted with carotid artery catheters were from Taconic Farms (New York, NY, USA). All animals were housed under specific-pathogen free conditions.

Human samples

The original ALI/ARDS study was approved by the Institutional Review Board of the University of Michigan Health System. In the current study, we used existing cryopreserved cell-free and anonymous bronchoalveolar lavage fluid (BALF) from mechanically ventilated patients that met criteria for ALI or ARDS by the European Respiratory Society/American Thoracic Society consensus definition (46). Details of patient enrollment, study protocol and BALF sampling techniques are described elsewhere (47). As controls, we used BALF samples from healthy, age-matched, medication-free, nonsmoking men and women. Western blotting of human BALF was done as described below.

ALI models

For LPS-ALI, mice were anesthetized, and 40 μl PBS containing 40 μg LPS (*Escherichia coli*, O111:B4; Sigma-Aldrich, St. Louis, MO, USA) injected intratracheally (i.t.; ref. 48). For immunoglobulin G immune complex (IgGIC)-ALI, mice received 125 μg rabbit anti-BSA IgG i.t. (MP Biomedicals, Solon, OH, USA), followed by 1 mg BSA i.v. (Sigma-Aldrich; ref. 48). Sham-treated mice received 40 μl PBS i.t. For C5a-ALI, mice received rmC5a (endotoxin level: <1.0 EU/μg protein; R&D Systems, Minneapolis, MN, USA). Histones for intratracheal administration were purified from calf thymus (Sigma-Aldrich). At the end of experiments, the lungs were flushed with 1 ml PBS to obtain BALF. After centrifugation (250 g, 5 min, 4°C), BALF cells were counted in a hemocytometer (Hausser Scientific, Horsham, PA, USA), and cell-free BALF was stored at −80°C until further analysis.

Measurement of histones, albumin, and mediator concentrations in BALF

Alveolar permeability was assessed by quantitative detection of mouse albumin in BALF by ELISA (Bethyl Laboratories, Montgomery, TX, USA). For detection of multiple mediators, the Bioplex Pro mouse cytokine assay, 23-Plex Group I (Bio-Rad, Richmond, CA, USA) was used on a Luminex-xMAP/Bioplex-200 System with Bioplex Manager 5.0 software. The following mediators were analyzed: IL-1α, IL-1β, IL-2, IL-3, IL-4, IL-5, IL-6, IL-9, IL-10, IL-12(p40), IL-12(p70), IL-13, IL-17, Eotaxin (CCL11), G-CSF, GM-CSF, IFN-γ, KC (CXCL1), MCP-1 (CCL2), MIP-1α (CCL3), MIP-1β (CCL4), RANTES (CCL5), and TNF-α. The ELISA for detection of histones (nucleosomes) in BALF was from Roche (Mannheim, Germany). Purified mixed calf thymus histones were used to generate standard curves.

Western blotting

For analysis of extracellular histones, mouse lungs were flushed with 4 × 1 ml PBS, BALF was centrifuged (400 g, 10 min, 4°C) and filtered (0.2-μm syringe filters, Fisher Scien-

tific, Waltham, MA, USA) and supernatants were stored at $-80°C$. BALFs from mice and humans were passed through Amicon filter tubes (EMD Millipore, Billerica, MA, USA) with a 30-kDa MW cutoff. The flow-through was then concentrated using 10-kDa MW cutoff filter tubes to a volume of 50 µl. This procedure enriched the BALF samples for proteins from 10 to 30 kDa. Proteins (40 µl of concentrated BALF) were separated by electrophoresis, transferred to nitrocellulose membranes, and probed with antibodies against histone H3 or histone H4 (Santa Cruz Biotechnology, Santa Cruz, CA, USA, and Millipore). Following staining with secondary antibodies conjugated to horseradish peroxidase (Amersham, Arlington Heights, IL, USA) the enzymatic reaction was visualized using chemiluminescent substrate (Denville Scientific, South Plainfield, NJ, USA). ImageJ 1.45s software (U.S. National Institutes of Health, Bethesda, MD, USA) was used for densitometry analysis of Western blots.

Flow cytometry

For detection of cell death we used the fixable viability dye eFluor450, and intracellular calcium was assessed using the calcium sensor dye eFluor514 (both from eBioscience, San Diego, CA, USA). Staining protocols were according to manufacturer's instructions. Events (5×10^4) were acquired on a BD LSR II flow cytometer (BD Biosciences, San Jose, CA, USA), and data were analyzed using FlowJo 7.6.4 software (TreeStar Inc., Ashland, OR, USA).

Microscopic imaging

Bright-field microscopy

Lungs were fixed in 4% formaldehyde overnight, and 3-µm paraffin-embedded sections were stained with hematoxylin and eosin (H&E). Cytospins of BALF cells were stained with modified Wright-Giemsa (Hema 3 Stain Set; Fisher Scientific). Digital images ($\times 40/0.9$, $\times 100/1.4$) were acquired using an Olympus BH2 microscope (Olympus, Center Valley, PA, USA).

Transmission electron microscopy

Lungs were fixed in 4% glutaraldehyde in 0.2 M cacodylate buffer, postfixed for 1 h hour in 1% osmium tetroxide, rinsed in cacodylate buffer, and dehydrated in ascending concentrations of ethanol. Next, samples were transitioned through propylene oxide and embedded in Epon epoxy resin (Momentive, Houston, TX, USA). Semithin sections were stained with toluidine blue for tissue identification. Selected regions of interest were ultrathin sectioned, 70 nm in thickness, and poststained with uranyl acetate and lead citrate. They were examined using a Philips CM100 electron microscope (Philips, Amsterdam, The Netherlands) at 60 kV. Images were recorded digitally using a Hamamatsu ORCA-HR digital camera (Hamamatsu Photonics, Hamamatsu, Japan) and AMT software (Advanced Microscopy Techniques Corp., Danvers, MA, USA).

Magnetic resonance imaging (MRI)

Animals were euthanized individually, and MRI examinations were completed within 10 min postmortem. Mice lay prone in a 7.0-T Agilent MR scanner (33 cm horizontal bore; Agilent, Palo Alto, CA, USA). The radiofrequency coils used to scan the thoracic region had a quadrature 35 mm volume for mice and 63 mm volume for rats, respectively. Axial proton density/ T_1-weighted images were acquired using a (fast) spin-echo sequence with the following parameters. Mice: repetition time (T_R)/effective echo time (T_E), 2000/11 ms; number of echoes, 8; field of view (FOV), 30×30 mm; matrix, 256×128; slice thickness, 1 mm; number of slices, 15 contiguous; and number of scans, 1 (total scan time ~4 min.). Rats: T_R/T_E, 3000/17 ms; number of echoes, 8; FOV, 70×70 mm; matrix, 256×128; slice thickness, 2 mm; number of slices, 20 contiguous; and number of scans, 1 (total scan time ~6.5 min.).

Whole-body plethysmography

A Buxco Max II and rodent bias flow supply part with unrestrained whole-body plethysmography chambers (all Buxco, Wilmington, NC, USA) were used. Rats were conditioned to being placed in the chambers for 1 wk before experiments. Physiological values from measured box flows were calculated using the Epstein algorithm (BioSystem XA for Windows 2.11 software; Buxco).

Blood gas analysis

Heparinized arterial blood (200–300 µl) was drawn from rats with carotid artery catheters and immediately analyzed on a Radiometer ABL 835 Flex Blood Gas Analyzer (Diamond Diagnostics, Holliston, MA, USA).

Cell culture

Alveolar epithelial cells, type II [mouse lung epithelial cell line 12 (MLE-12) and mouse lung adenoma cell line 4 (LA-4)] were a gift from Dr. J. B. Weinberg (University of Michigan). MLE-12 cells were cultured in RPMI1640 (10% FCS, 100 U/ml penicillin-streptomycin, 2 mM L-glutamine, 10 mM HEPES, 10 nM β-estradiol, 10 nM hydrocortisone, 5 µg/ml transferrin, and 1× insulin-transferrin-selenite) and LA-4 cells in DMEM (15% FCS, 100 U/ml penicillin-streptomycin, and 2 mM L-glutamine).

Antibodies and reagents

The following reagents were used: anti-Ly6G antibody (clone RB6-8C5) and rat IgG2bκ isotype antibody (eBioscience), neutralizing anti-histone H4 antibody (clone BWA3; ref. 49) and mouse IgG1κ isotype antibody (BioLegend), rmC5a (R&D Systems), purified histones from calf thymus (Sigma), histone H1 and histone H3 (Roche), and histone H4 (BPS Bioscience, San Diego, CA, USA). The lactate dehydrogenase (LDH) assay kit (Cayman Chemical, Ann Arbor, MI, USA) was used according to instructions by the manufacturer.

Statistical analysis

GraphPad Prism 5.04 software (GraphPad, San Diego, CA, USA) was used for statistical analysis. All values are expressed as means, and error bars represent SEM. Data sets were analyzed by 2-tailed Student's t test or 1-way ANOVA. *In vitro* experiments were performed independently ≥ 3 times, and *in vivo* experiments used numbers of mice as indicated in the figure legends. Values of $P < 0.05$ were considered significant.

RESULTS

### Dependency in ALI on both C5aR and C5L2

To investigate the respective roles of C5aR and C5L2 *in vivo* in C57BL/6J mice, we used the genetically manipulated (knockout) or nonmanipulated mouse strains in three types of ALI (LPS, IgGIC, and C5a). The severity of ALI was assessed by ELISA quantification of albumin leakage in BALF as a marker in loss of epithelial/endothelial (alveolar) barrier function. When $C5aR^{-/-}$ and $C5L2^{-/-}$ mice were compared to C57BL/6J wild-type (Wt) mice after LPS-ALI, increases in alveolar permeability were substantially reduced with genetic absence of either C5a receptor (**Fig. 1A**). The severity of lung injury was also reduced following IgGIC-ALI in both $C5aR^{-/-}$ and $C5L2^{-/-}$ mice (Fig. 1B). Similar patterns were obtained when ALI was induced by intratracheal administration of recombinant mouse C5a (C5a-ALI, Fig. 1C). The levels of alveolar albumin in $C5aR^{-/-}$ and $C5L2^{-/-}$ mice after C5a-ALI remained at concentrations comparable to C57BL/6J (Wt) mice after PBS i.t. (sham treatment), whereas the same dose of C5a resulted in extensive injury in C57BL/6J (Wt) mice (Fig. 1C). BALF cells from C5a-ALI experiments demonstrated the expected abundance of PMNs in C57BL/6J (Wt) mice (Fig. 1D, top right panel). Many fewer PMNs were present in BAL preparations obtained from $C5L2^{-/-}$ mice, and low numbers of alveolar macrophages were present in samples from $C5aR^{-/-}$ mice and in sham-treated C57BL/6J (Wt) mice (Fig. 1D). Quantitative counts of BALF PMNs after C5a-ALI from the three mouse strains and Wt shams are shown (Fig. 1E). Histopathology of lung sections from C57BL/6J (Wt), $C5aR^{-/-}$ and $C5L2^{-/-}$ mice after C5a-ALI demonstrated suppression of the inflammatory response and injury with genetic deficiency of either of the two C5a receptors (Fig. 1F).

Presence of extracellular histones in lungs from humans with ALI

Recent findings have suggested a role of histones released into the vascular compartment in the setting of sepsis in subhuman primates (50). To determine the presence of extracellular histones during ALI, we screened cryopreserved cell-free BALF samples from healthy volunteers ($n=12$) and human patients with ALI/ARDS ($n=21$). Serial BALF samples from each patient with ALI, using sequential time points (d 0–22) after diagnosis of ALI/ARDS were available ($n=52$ samples in total). The demographics of the study population are shown in Supplemental Table S1. The ALI/ARDS patients were critically ill, requiring mechanical ventilation. Bacterial pneumonia and sepsis were most commonly identified as the precipitating event leading to ALI/ARDS.

Examples of Western blot analysis for presence of H4
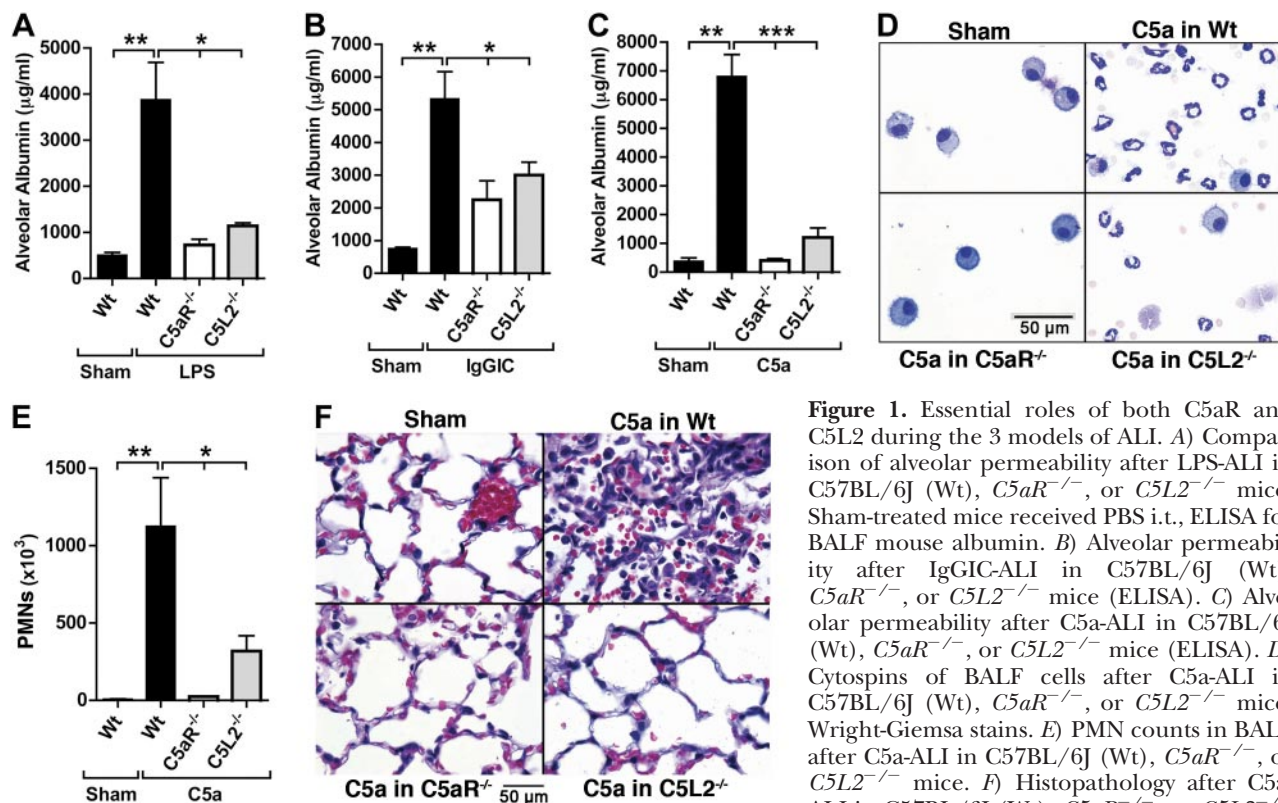
Figure 1. Essential roles of both C5aR and C5L2 during the 3 models of ALI. *A*) Comparison of alveolar permeability after LPS-ALI in C57BL/6J (Wt), $C5aR^{-/-}$, or $C5L2^{-/-}$ mice. Sham-treated mice received PBS i.t., ELISA for BALF mouse albumin. *B*) Alveolar permeability after IgGIC-ALI in C57BL/6J (Wt), $C5aR^{-/-}$, or $C5L2^{-/-}$ mice (ELISA). *C*) Alveolar permeability after C5a-ALI in C57BL/6J (Wt), $C5aR^{-/-}$, or $C5L2^{-/-}$ mice (ELISA). *D*) Cytospins of BALF cells after C5a-ALI in C57BL/6J (Wt), $C5aR^{-/-}$, or $C5L2^{-/-}$ mice, Wright-Giemsa stains. *E*) PMN counts in BALF after C5a-ALI in C57BL/6J (Wt), $C5aR^{-/-}$, or $C5L2^{-/-}$ mice. *F*) Histopathology after C5a-ALI in C57BL/6J (Wt), $C5aR^{-/-}$, or $C5L2^{-/-}$ mice (H&E stains). Duration of all ALIs shown was 8 h, and 500 ng i.t. rmC5a was used for C5a-ALI. Data from each experiment shown are representative of $n \geq 7$ mice/group. Error bars = SEM. *$P < 0.05$, **$P < 0.01$, ***$P < 0.001$; Student's *t* test.

in BALF from patients with ALI are shown in **Fig. 2A**, top panel. Figure 2A features a control (healthy volunteer) BALF showing absence of reactivity for histone 4 in the 15-kDa region. Patient 40589 BALF samples, from a patient with ALI, were obtained at d 5, 14, and 21, revealing H4 reactivity near the 15-kDa position at all time points. Patient 50131 BALF samples were also consecutively obtained from a patient with ALI, and H4 presence was found on d 4, but not on d 8 and 21. It would appear that H4 presence in BALF from patients with ALI may be sustained or transient.

The presence of histone H4 in BALF from all samples of patients with ALI/ARDS and healthy volunteers was determined by Western blotting, and results were categorized as either positive or negative (Fig. 2A, bottom panel). Analysis of $n = 12$ samples of patients with ALI/ARDS collected between d 0 and 5 after diagnosis of ALI revealed that 50% of BALF samples contained histone H4 (Fig. 2A, bottom panel, left bar).

Lower rates of histones were present in BALF samples collected later than d 10 after ALI/ARDS diagnosis. In BALF from healthy volunteers (control, $n=12$) histone H4 was not detectable (Fig. 2A, bottom panel).

Appearance of histones during experimental ALI is dependent on C5aR, C5L2, and PMNs

To further assess the relevance of extracellular histones, we analyzed murine BALF from three experimental models of ALI. Histone H3 and histone H4 were both detectable by Western blotting in cell-free BALF from C57BL/6J mice after LPS-ALI, IgGIC-ALI, and C5a-ALI (Fig. 2B, top panel). Both C5a receptors (C5aR and C5L2) were required to generate extracellular histones in C5a-ALI (Fig. 2B, bottom panel).

C5a is known to have chemotactic activity for PMNs (7). To investigate what cell type is required for mediating the appearance of extracellular histones during
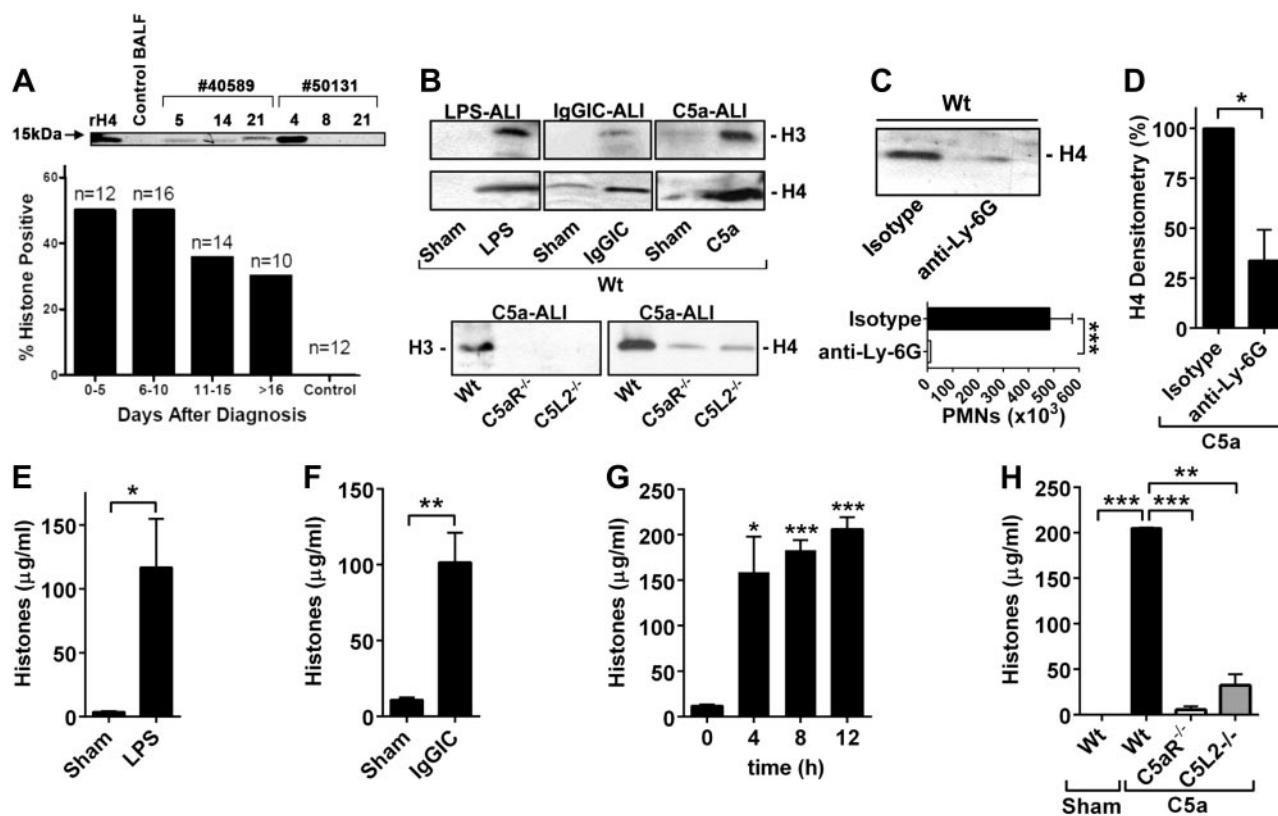
Figure 2. Detection of extracellular histones during ALI in humans or mice. *A*) Top panel: Western blotting of histone H4 in BALF from 2 humans with ALI/ARDS (40589; 50131) at sequential time points (4–21 d), a healthy volunteer (Ctrl BALF, negative control), or recombinant H4 (rH4, positive control). Bottom panel: presence of histone H4 in BALF from humans with ALI/ARDS and healthy volunteers (Western blotting). Percentage values of positive samples are indicated as bars for different time points after diagnosis of ALI/ARDS, with total numbers of analyzed samples at top of each bar. *B*) Histones H3 and H4 in BALF after ALI models in Wt, $C5aR^{-/-}$, or $C5L2^{-/-}$ mice, 8 h; Western blotting. *C*) Top panel: histone H4 detection by Western blotting in BALF of PMN-depleted Wt mice 8 h after C5a-ALI. Depletion of PMNs was achieved by monoclonal anti-Ly-6G antibody (200 μg i.p., −24 h) using isotype IgG as control. Bottom panel: absence of BALF PMNs after anti-Ly-6G treatment. *D*) Densitometry of three independent Western blots for histone H4 in BALF of C5a-ALI (8 h) in Wt mice, when PMNs were depleted as described above. *E*) ELISA for extracellular histones in BALF of sham-treated Wt mice or in Wt mice after LPS-ALI, 8 h. *F*) Extracellular histones in BALF after IgGIC-ALI in Wt mice, 8 h; ELISA. *G*) Time course of histone release in BALF following C5a-ALI, ELISA. *H*) Detection of extracellular histones in BALF of Wt, $C5aR^{-/-}$ and $C5L2^{-/-}$ mice after C5a-ALI, 8 h; ELISA. Data are representative of the indicated numbers of human samples (*A*) or $n = 5$ mice/group (*B–H*). Error bars = SEM. *$P < 0.05$; Student's *t* test.
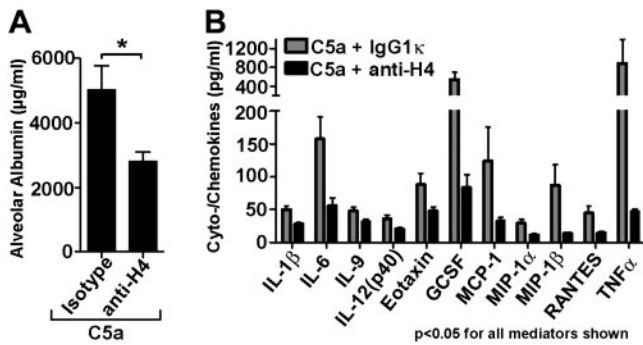
Figure 3. Protective effects of neutralization of extracellular histones during ALI. *A*) Reduced alveolar permeability disturbances after C5a-ALI with treatment of neutralizing anti-H4 antibody (BWA3, 250 µg i.v. + 50 µg i.t.) or isotype control IgG1κ, 8 h; ELISA. *B*) Multiplex bead-based assay of mediators in BALF after C5a-ALI with treatment of anti-H4 antibody or control IgG1κ, 8 h; ELISA. Only mediators with significant differences ($P<0.05$, 11 of 23 mediators) between groups are shown. C5a was used as 500 ng/mouse i.t. Data were acquired using $n \geq 15$ mice/group. Error bars = SEM. *$P < 0.05$; Student's *t* test.

C5a-ALI, we depleted Ly-6G$^+$ PMNs using monoclonal antibody (Fig. 2*C*). The amount of histone H4 in cell-free BALF after C5a-ALI was sharply reduced (Fig. 2*C*, top panel) when blood PMNs were depleted by >90% following treatment with anti-Ly-6G as compared to IgG isotype control antibody (Fig. 2*C*, bottom panel). Densitometry analysis of Western blot films of PMN-depleted BALF showed a reduction of nearly 75% in histone H4 (Fig. 2*D*).

To confirm our findings on release of extracellular

histones in the models of ALI, we used an ELISA reactive for histones H1, H2A, H2B, H3, and H4. Histones in BALF were abundant following induction of ALI by LPS or immune complexes (Fig. 2*E, F*). Time-ourse studies revealed that histones were present in BALF as early as 4 h after C5a-ALI (Fig. 2*G*). Finally, histones were greatly reduced (85–95%) after C5a-ALI in $C5aR^{-/-}$ mice and $C5L2^{-/-}$ mice, as detected by ELISA of BALF (Fig. 2*H*).

Blockade of extracellular histones attenuates severity of ALI

To study the biological relevance of extracellular histones during C5a-ALI, a neutralizing anti-histone H4 antibody was given simultaneously with intratracheal instillation of C5a into C57BL/6J lungs ($n=15$). The control group ($n=16$) received a matched preservative-free isotype IgG1κ. Blockade of extracellular histone H4 significantly ($P=0.0125$) reduced by ~50% the severity of alveolar barrier disruption following C5a-ALI (**Fig. 3*A***). Analysis of BALF from C5a-ALI experiments with anti-histone H4 treatment also revealed greatly reduced release of many proinflammatory mediators (Fig. 3*B*), including TNF-α and IL-6, as well as chemokines, such as MCP-1, MIP-1α, and MIP-1β.

## Extracellular histones are cytotoxic for alveolar epithelial cells

To evaluate the mechanistic effects of extracellular histones during lung injury, cultures of mouse MLE-12 and LA-4 cells were employed. Both cell lines are
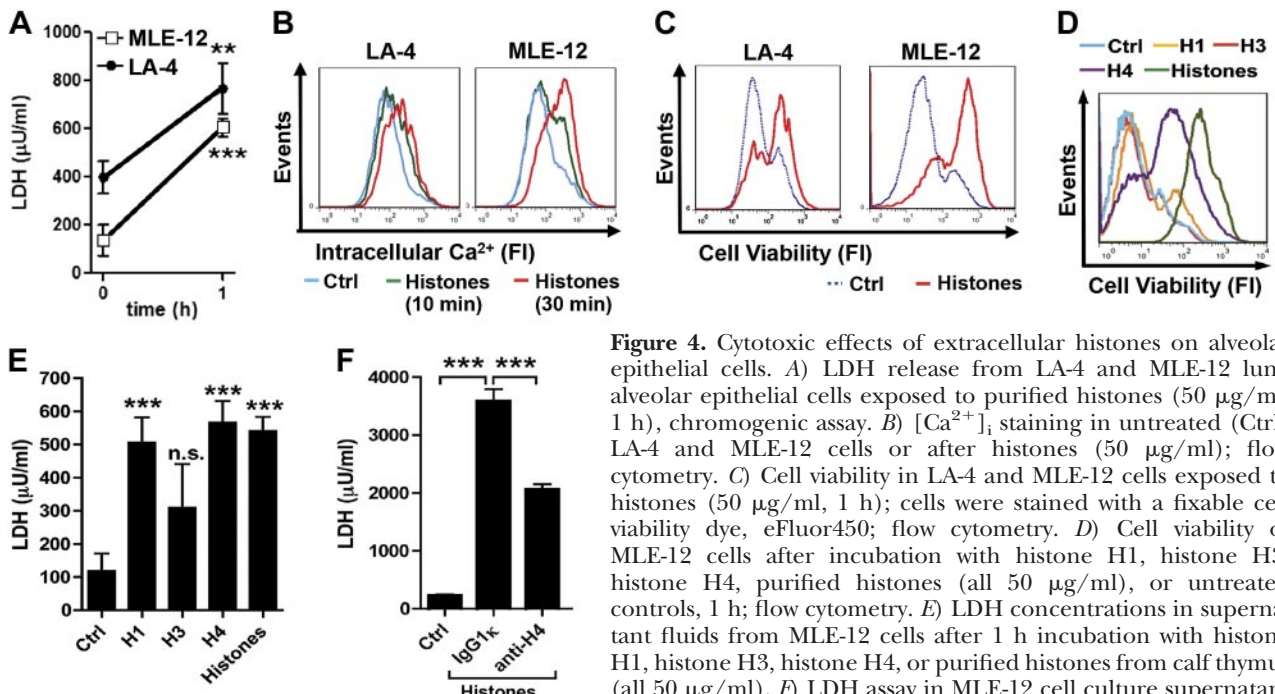
Figure 4. Cytotoxic effects of extracellular histones on alveolar epithelial cells. *A*) LDH release from LA-4 and MLE-12 lung alveolar epithelial cells exposed to purified histones (50 µg/ml, 1 h), chromogenic assay. *B*) $[Ca^{2+}]_i$ staining in untreated (Ctrl) LA-4 and MLE-12 cells or after histones (50 µg/ml); flow cytometry. *C*) Cell viability in LA-4 and MLE-12 cells exposed to histones (50 µg/ml, 1 h); cells were stained with a fixable cell viability dye, eFluor450; flow cytometry. *D*) Cell viability of MLE-12 cells after incubation with histone H1, histone H3, histone H4, purified histones (all 50 µg/ml), or untreated controls, 1 h; flow cytometry. *E*) LDH concentrations in supernatant fluids from MLE-12 cells after 1 h incubation with histone H1, histone H3, histone H4, or purified histones from calf thymus (all 50 µg/ml). *F*) LDH assay in MLE-12 cell culture supernatant fluids. MLE-12 cells were left as untreated controls or incubated for 60 min with purified histones (12.5 µg/ml) premixed (30 min, 37°C) with either IgG1κ isotype control antibody (250 µg/ml) or anti-histone H4 antibody (BWA3; 250 µg/ml). Data are representative of 3 independent experiments. Error bars = SEM. n.s., not significant. **$P < 0.01$, ***$P < 0.001$; Student's *t* test.
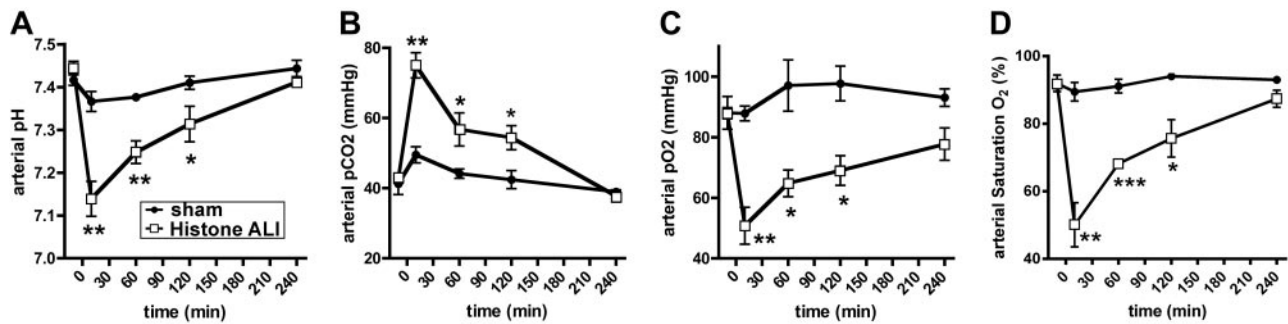
Figure 5. Administration of extracellular histones into airways induces severe disturbances in alveolar-capillary gas exchange. Purified histones (50 µg/g body weight) were administered i.t. to Sprague-Dawley rats with implanted carotid artery catheters. Sham-treated animals only received PBS i.t. Serial blood gas analyses were performed at baseline and at intervals following the intervention. *A*) Arterial pH. *B*) Arterial pCO_2. *C*) Arterial pO_2. *D*) Arterial oxygen saturation, $SatO_2$. Data are representative of $n \geq 4$ rats/group. Error bars = sem. *$P < 0.05$, **$P < 0.01$, ***$P < 0.001$; Student's *t* test.

known to display phenotypic characteristics of type II alveolar epithelial cells (*e.g.*, surfactant production). Incubation of either cell type with purified calf thymus histones caused release within 1 h of LDH in supernatant fluids, indicating cell death (**Fig. 4*A***). Flow cytometry studies revealed a rise in intracellular Ca^{2+} levels in response to histone exposure in MLE-12 and LA-4 cells at both 10 and 30 min (Fig. 4*B*). Consistent with the rise of LDH, fluorescent staining techniques of MLE-12 and LA-4 cells after the histone mixture indicated decreased cell viability (Fig. 4*C*). Distinct cytotoxic activities of histone H1, histone H3, and histone H4 were seen at 60 min when compared to purified histones (mixture of histone proteins; Fig. 4*D*, *E*). Notably, the neutralizing anti-histone H4 antibody used in C5a-ALI experiments (Fig. 3*A*, *B*) was also protective in cultures of MLE-12 cells when incubated with purified histones (Fig. 4*F*).

Extracellular histones compromise lung function by tissue damage and promotion of inflammation

To further characterize the effects of extracellular histones *in vivo*, purified histones were instilled into the airways of Sprague-Dawley rats. Such treatments resulted in immediate, severe respiratory disturbances with compromised lung ventilation patterns, cyanosis and occasional death. Serial blood gas analysis of rats after intratracheal administration of histones compared to sham treatment (PBS i.t.) showed a substantial acidification in arterial pH (**Fig. 5*A***) together with greatly elevated carbon dioxide tension (pCO_2) (Fig. 5*B*). In addition, arterial oxygen tension and arterial oxyhemoglobin saturation (SaO_2) were severely reduced after histone administration (Fig. 5*C*, *D*). Values for arterial base excess (BE; 0.8 ± 0.6 *vs.* -0.8 ± 0.8 mM) and arterial bicarbonate (HCO_3^-: 26.0 ± 0.5 *vs.* 25.4 ± 0.5
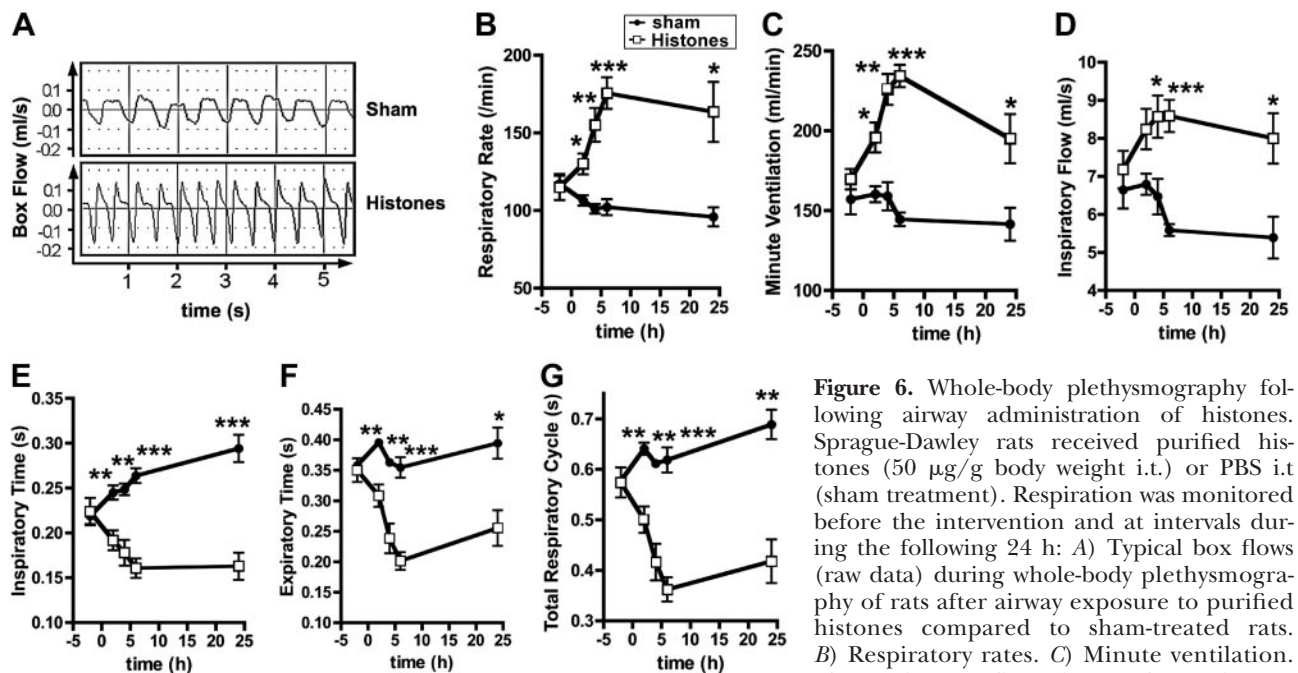
Figure 6. Whole-body plethysmography following airway administration of histones. Sprague-Dawley rats received purified histones (50 µg/g body weight i.t.) or PBS i.t (sham treatment). Respiration was monitored before the intervention and at intervals during the following 24 h: *A*) Typical box flows (raw data) during whole-body plethysmography of rats after airway exposure to purified histones compared to sham-treated rats. *B*) Respiratory rates. *C*) Minute ventilation. *D*) Inspiratory flow times. *E*) Inspiratory times. *F*) Expiratory flow times. *G*) Total respiratory cycle. Data are representative of $n \geq 4$ rats/group. Error bars = sem. *$P < 0.05$, **$P < 0.01$, ***$P < 0.001$; Student's *t* test.

mM) remained within normal limits in both groups (data not shown). Collectively, arterial blood gas analyses after histone treatment reflected acute disturbances in gas exchange across the alveolar-capillary membranes, leading to severe respiratory acidosis.

Lung ventilation was also assessed by whole-body plethysmography. Box flows (raw data) of lung excursions from rats following histone administration displayed obvious functional abnormalities (**Fig. 6A**). There were steep increases in respiratory rates (Fig. 6B), minute ventilation (Fig. 6C), and inspiratory flow (Fig. 6D) in response to intratracheal purified histones. In accordance with the increased respiratory rates, inspiratory times (Fig. 6E), expiratory times (Fig. 6F) and total respiratory cycle times (Fig. 6G) were greatly diminished. The abnormalities in lung ventilation patterns (Fig. 6) persisted for 24 h and may in part account for a compensatory normalization of blood gases at the later time points (Fig. 5).

The administration of calf thymus histones into airways of C57BL/6J mice resulted in dose-dependent disruption of the alveolar permeability barrier (**Fig. 7A**). The peak in alveolar albumin leakage occurred 8 h after histone instillation (Fig. 7B). Leukocytes [white blood cells (WBCs)] were > 80% PMNs, peaking at 8 h (Fig. 7C). The early suppression of WBCs at the 1 and 3 h time points may be explained by the rapid cytotoxic effects of histones, triggering a wave of migration of inflammatory cells into the alveolar compartment at time points ≥6 h (Fig. 7C). The cytotoxicity of histones given *via* the airways was documented by an early increase of LDH levels in BALF (Fig. 7D). A time-dependent
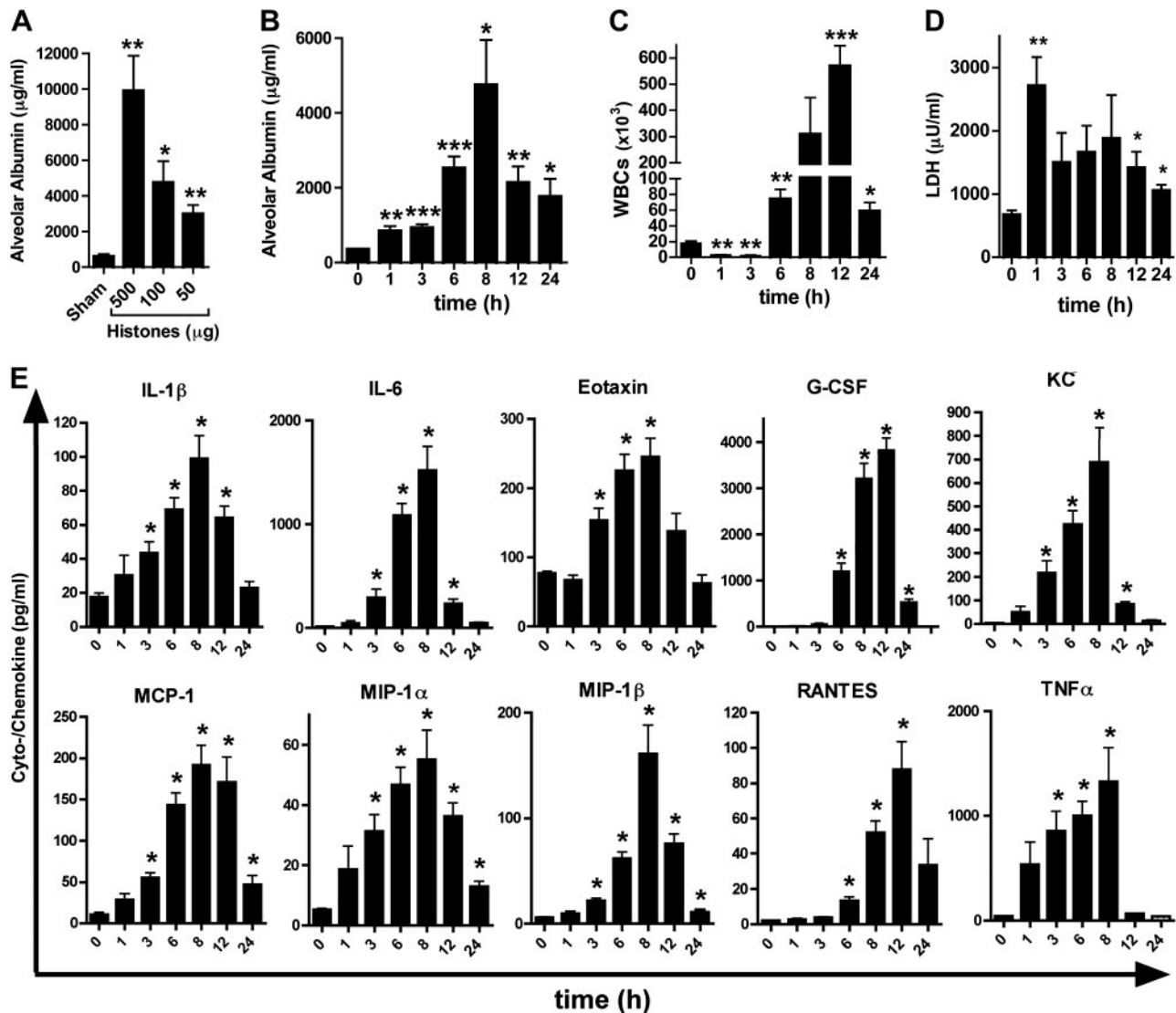
Figure 7. Induction of acute inflammation in lungs by extracellular histones. *A*) Disruption of alveolar permeability in C57BL/6J mice after intratracheal deposition of purified histones at different doses, 8 h; BALF albumin ELISA. *B*) Time course for alveolar permeability after exposure to purified histones (100 µg i.t.), C57BL/6J mice; ELISA. *C*) White blood cell (WBC) content (mainly PMNs) in BALF from C57BL/6J mice after purified histones from the experiment described in *B*. *D*) LDH in BALF from the experiment in *B*; chromogenic assay. *E*) Mediators in C57BL/6J mice after treatment with purified histones (100 µg i.t.), with BALF harvested at different time points; multiplex bead-based assay. Data are representative of $n \geq 5$ mice/group. Error bars = SEM. *$P < 0.05$, **$P < 0.01$, ***$P < 0.001$; Student's *t* test.

release of several proinflammatory cytokines (IL-1β, IL-6, and TNF-α) and chemokines (KC, MCP-1, MIP-1α, MIP-1β, and RANTES) occurred following administration of histones i.t. (Fig. 7E). Several of these mediators, such as IL-1β, IL-6, and TNF-α, are known to be associated with development and progression of ARDS in humans (4, 5). Administration of histone extracts to $C5aR^{-/-}$ mice did not result in less severity of ALI or less PMN influx, suggesting that there is no feedback of extracellular histones on complement activation (Supplemental Fig. S1). Therefore, once formed, histones do not require C5aR or C5L2 for induction of ALI.

High-resolution MRI was employed for imaging of lungs following administration of histones i.t. (**Fig. 8A, B**). Axial thoracic images showed bilateral signal-intense lung infiltrates consistent with pulmonary edema in both C57BL/6J (Wt) mice and Sprague-Dawley rats (Fig. 8A, B, arrowheads), which were not seen in sham-treated controls. The technical imaging quality was superior in Sprague-Dawley rats as compared to smaller scale mouse lungs. More detailed MRI scans (z stacks) of rat lungs are available in Supplemental Videos S1 and S2.

Histopathologic examination of lungs after histone instillation showed accumulation of PMNs in alveolar spaces, capillary congestion, and areas of intra-alveolar hemorrhage, fibrin deposits and thrombi (especially in large veins), together with exfoliation of bronchial epithe-

lial cells and increased mucous production by epithelial cells (Fig. 8C). Transmission electron micrographs demonstrated normal vasculature and airway architecture in sham-treated mice (Fig. 8D, top and bottom left panels). Following lung exposure to histones, intra-alveolar PMNs, erythrocytes, fibrin deposits (arrow heads) and epithelial cell injury with bleb formation (arrow) were observed (Fig. 8D, top and bottom right panels).
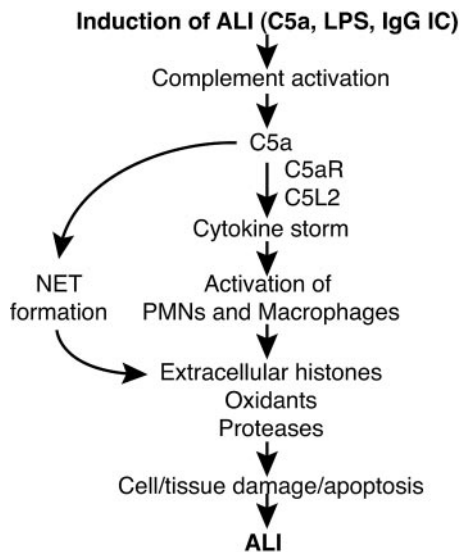
In summary, ALI induced by LPS, IgGIC or C5a caused release of histones in the distal alveolar compartment. Histones were directly cytotoxic for various lung cell types, especially alveolar epithelial cells, promoting subsequent ALI and persistent inflammation.

DISCUSSION

The occurrence of tissue injury and cell death is a common feature of many acute and chronic inflammatory diseases, including those involving the lung. This phenomenon translates into organ dysfunction that may be followed by either tissue remodeling with fibrosis or persistent organ failure. Our findings characterize the molecular events connecting anaphylatoxin C5a and its receptors with the manifestations of organ failure occurring in animals or patients with ALI/ARDS (**Fig. 9**).
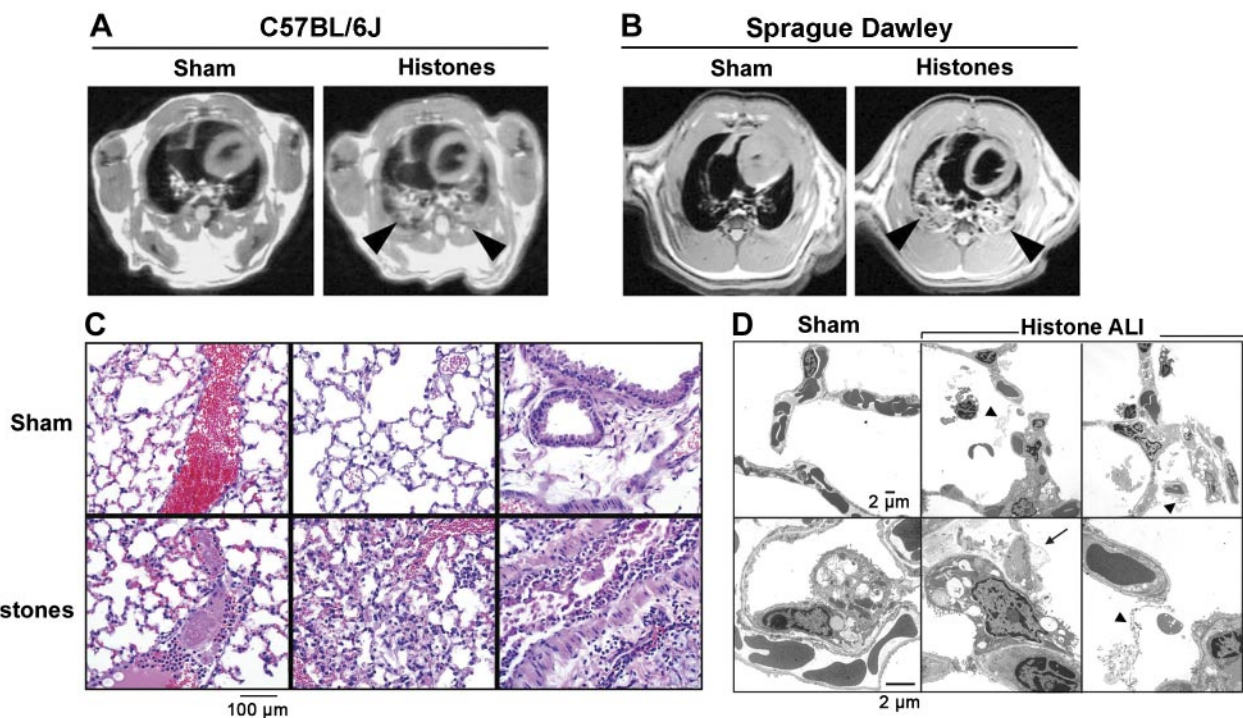
Figure 8. Extracellular histones mediate lung consolidation and acute histopathology in lungs. *A*) High-resolution MRI of lungs from C57BL/6J mice after PBS i.t. (sham treatment) or purified histones (20 µg/g body weight), 6 h. Arrowheads indicate signal-intense intrapulmonary areas consistent with consolidation of lung tissue; axial proton density/T1-weighted images; slice thickness: 1 mm. *B*) High-resolution MRI of lungs from Sprague-Dawley rats 6 h after PBS i.t. (sham) or purified histones (20 µg/g body weight). Arrowheads indicate signal-intense intrapulmonary areas of lung infiltrations; slice thickness: 2 mm. *C*) Histopathology of lungs from C57BL/6J mice after treatment with purified histones (20 µg/g body weight i.t.) compared to sham-treated lungs, 6 h, H&E staining. *D*) Transmission electron microscopy of normal lungs (sham treatment) from C57BL/6J mice compared to lungs after exposure to purified histones (100 µg i.t.), 8 h; ×2000. Arrow indicates blebbing of type II pneumocyte; arrowheads indicate fibrin deposits. Data are representative of $n \geq 5$ animals/group.

Induction of ALI (C5a, LPS, IgG IC)

Complement activation

↓

C5a
C5aR
C5L2

Cytokine storm

NET
formation

Activation of
PMNs and Macrophages

→ Extracellular histones
Oxidants
Proteases

Cell/tissue damage/apoptosis

ALI

Figure 9. Schematic overview of the proposed pathophysiologic events in ALI. LPS and IgG immune complexes trigger complement activation, including release of C5a. Ligation of C5a with C5aR and C5L2 activates PMNs and macrophages for mediating the formation of NETs in the case of PMNs. Extracellular histones derived from NETs or dying nonleukocytic cells perpetuate detrimental cell/tissue injury, resulting in greater severity of ALI.

C5a orchestrates immediate innate immune defense mechanisms to facilitate clearance of pathogens and harmful noninfectious agents [damage-associated molecular patterns (DAMPs) and alarmins]. To our surprise, instillation of recombinant C5a into the airways of mice did not require a costimulus to initiate damaging inflammation, consistent in part with findings that used rabbits and human C5a purified from activated serum decades ago (51). Injection of C5a has been used recently to induce peritonitis in mice (52). C5L2, in addition to C5aR, is required for full C5a-dependent activation of signaling pathways in Ly-6G$^+$ PMNs (30). Genetic deficiency of either C5aR or C5L2 markedly reduced the intensity of ALI in all models tested, as reported herein. This may suggest functional cooperation between C5aR and C5L2 (53), implying that C5aR cannot compensate for the absence of C5L2, and *vice versa.* We were unable to confirm an earlier report of anti-inflammatory properties of C5L2 during IgGIC-ALI (45). These apparent discrepancies may be explained by variations in methodologies regarding dosing and species (chicken *vs.* bovine) of the albumins and anti-albumin antibodies, as well as differences in the genetic backgrounds of C5L2-deficient mice. Notably, our findings are in accordance with a recent report describing proinflammatory roles of C5L2 in the context of experimental asthma (33).

Our findings suggest that the detrimental effects of complement activation during experimental lung injury are associated with release of histones into the lung. In addition, we also show the presence of extracellular histones in BALF in approximately half of human patients with ALI/ARDS. In our experiments,

histones outside of cells were highly cytotoxic for alveolar epithelial cells, promoting tissue damage and inflammation; such effects were reversed by blockade of histones *in vivo.* Emerging evidence suggests that complement activation may trigger the appearance of nucleosomes (histones/DNA) after trauma and appearance of NETs during viral infection (54, 55). Of note, several other endogenous cytotoxic factors are known. The intravital lysis of erythrocytes or muscle fibers with release of free hemoglobin or myoglobin often results in nephrotoxicity (56). Recently, the leakage of components from mitochondria to areas beyond has been linked to induction of inflammation (57). Another group has suggested that appearance of extracellular histones (in plasma) is associated with death in experimental sepsis in rodents and subhuman primates (50). Extracellular histones in the vasculature were found to be cytotoxic for the endothelium (50). A recent study has linked circulating histones with trauma-associated ALI/ARDS (58).

In the era following the discovery of penicillin, histone extracts were recognized to have bactericidal activity *in vitro* (59). Recombinant histone H4 possesses antimicrobial activity against *Staphylococcus aureus* and *Propionibacterium acnes* (60). Histones can be released from dying nonimmune cells and inhibit uptake of apoptotic cell particles by phagocytes (61, 62). The bactericidal potential of histones may be advantageous to the formation of NETs that capture and remove bacteria as part of innate immune defenses triggered by TLR4 on platelets (38, 43, 63). On the other hand, NETs directly promote cell death of nonleukocytic cells (64), which may trigger an additional release of histones from these cells. Histone H3 has been reported to interfere with the phagocytosis of apoptotic cells by macrophages (62). These concepts are shown in Fig. 9. The effects of extracellular histones in murine models of liver injury are dependent on TLR2 and TLR4 receptors (65). However, extracellular histones have direct cytotoxic activities not only on eukaryotic cells but also prokaryotes, the latter not expressing Toll-like receptors. In our experiments lung injury induced by extracellular histones was also reduced in *TLR4$^{-/-}$* mice (data not shown). In addition to these mechanisms, we present novel evidence that full release of extracellular histones requires the presence of C5aR and C5L2 receptors (Fig. 2).

Extracellular histones appear to undergo cleavage by activated protein C (APC), resulting in their inactivation (50). APC was the only drug approved by the FDA for the treatment of sepsis until its recent withdrawal from the market. Therefore, more effective strategies for the blockade of extracellular histones are needed. Death of alveolar epithelial cells during lung inflammation may result from or augment the release of cytotoxic histones which subsequently trigger adjacent cells (endothelial, alveolar epithelial cells) to undergo disintegration. During ALI, pharmacologic enhancement of apoptosis may induce less cytotoxic outcomes due to reduced release of histones. Whether histones could be

reduced by transfusion of mesenchymal stem cells, which have been proposed as a novel treatment for ALI, remains a matter of speculation (66). The concept that complement activation *via* C5aR and C5L2 triggers release of products of nucleosomes (such as histones), resulting in a circle of tissue injury and inflammation, in the setting of ALI and other diseases, deserves further study. **FJ**

REFERENCES

1. Goss, C. H., Brower, R. G., Hudson, L. D., and Rubenfeld, G. D. (2003) Incidence of acute lung injury in the United States. *Crit. Care Med.* **31**, 1607–1611
2. Rubenfeld, G. D., Caldwell, E., Peabody, E., Weaver, J., Martin, D. P., Neff, M., Stern, E. J., and Hudson, L. D. (2005) Incidence and outcomes of acute lung injury. *N Engl. J. Med.* **353**, 1685–1693
3. Erickson, S. E., Martin, G. S., Davis, J. L., Matthay, M. A., and Eisner, M. D. (2009) Recent trends in acute lung injury mortality: 1996–2005. *Crit. Care Med.* **37**, 1574–1579
4. Matthay, M. A., Ware, L. B., and Zimmerman, G. A. (2012) The acute respiratory distress syndrome. *J. Clin. Invest.* **122**, 2731–2740
5. Matthay, M. A., and Zemans, R. L. (2011) The acute respiratory distress syndrome: pathogenesis and treatment. *Ann. Rev. Pathol.* **6**, 147–163
6. Huber-Lang, M., Sarma, J. V., Zetoune, F. S., Rittirsch, D., Neff, T. A., McGuire, S. R., Lambris, J. D., Warner, R. L., Flierl, M. A., Hoesel, L. M., Gebhard, F., Younger, J. G., Drouin, S. M., Wetsel, R. A., and Ward, P. A. (2006) Generation of C5a in the absence of C3: a new complement activation pathway. *Nat. Med.* **12**, 682–687
7. Bosmann, M., and Ward, P. A. (2012) Role of C3, C5 and anaphylatoxin receptors in acute lung injury and in sepsis. *Adv. Exp. Med. Biol.* **946**, 147–159
8. Sun, L., Guo, R. F., Gao, H., Sarma, J. V., Zetoune, F. S., and Ward, P. A. (2009) Attenuation of IgG immune complex-induced acute lung injury by silencing C5aR in lung epithelial cells. *FASEB J.* **23**, 3808–3818
9. Martin, T. R., and Matute-Bello, G. (2011) Experimental models and emerging hypotheses for acute lung injury. *Crit. Care Clin.* **27**, 735–752
10. Ward, P. A. (2003) Acute lung injury: how the lung inflammatory response works. *Eur. Respir. J. Suppl.* **44**, 22s–23s
11. Martin, T. R., Hagimoto, N., Nakamura, M., and Matute-Bello, G. (2005) Apoptosis and epithelial injury in the lungs. *Proc. Am. Thorac. Soc.* **2**, 214–220
12. Gao, H., Neff, T., and Ward, P. A. (2006) Regulation of lung inflammation in the model of IgG immune-complex injury. *Ann. Rev. Pathol.* **1**, 215–242
13. Warren, J. S., Yabroff, K. R., Remick, D. G., Kunkel, S. L., Chensue, S. W., Kunkel, R. G., Johnson, K. J., and Ward, P. A. (1989) Tumor necrosis factor participates in the pathogenesis of acute immune complex alveolitis in the rat. *J. Clin. Invest.* **84**, 1873–1882
14. Ricklin, D., Hajishengallis, G., Yang, K., and Lambris, J. D. (2010) Complement: a key system for immune surveillance and homeostasis. *Nat. Immunol.* **11**, 785–797
15. Guo, R. F., and Ward, P. A. (2005) Role of C5a in inflammatory responses. *Ann. Rev. Immunol.* **23**, 821–852
16. Sarma, J. V., and Ward, P. A. (2011) The complement system. *Cell Tissue Res.* **343**, 227–235
17. Webster, R. O., Larsen, G. L., and Henson, P. M. (1982) In vivo clearance and tissue distribution of C5a and C5a des arginine complement fragments in rabbits. *J. Clin. Invest.* **70**, 1177–1183
18. Gerard, C., and Gerard, N. P. (1994) C5A anaphylatoxin and its seven transmembrane-segment receptor. *Ann. Rev. Immunol.* **12**, 775–808
19. Gerard, N. P., and Gerard, C. (1991) The chemotactic receptor for human C5a anaphylatoxin. *Nature* **349**, 614–617
20. Bosmann, M., Haggadone, M. D., Hemmila, M. R., Zetoune, F. S., Sarma, J. V., and Ward, P. A. (2012) Complement activation product C5a is a selective suppressor of TLR4-induced, but not TLR3-induced, production of IL-27(p28) from macrophages. *J. Immunol.* **188**, 5086–5093
21. Lalli, P. N., Strainic, M. G., Yang, M., Lin, F., Medof, M. E., and Heeger, P. S. (2008) Locally produced C5a binds to T cell-expressed C5aR to enhance effector T-cell expansion by limiting antigen-induced apoptosis. *Blood* **112**, 1759–1766
22. Strainic, M. G., Liu, J., Huang, D., An, F., Lalli, P. N., Muqim, N., Shapiro, V. S., Dubyak, G. R., Heeger, P. S., and Medof, M. E. (2008) Locally produced complement fragments C5a and C3a provide both costimulatory and survival signals to naive CD4+ T cells. *Immunity* **28**, 425–435
23. Riedemann, N. C., Guo, R. F., Sarma, V. J., Laudes, I. J., Huber-Lang, M., Warner, R. L., Albrecht, E. A., Speyer, C. L., and Ward, P. A. (2002) Expression and function of the C5a receptor in rat alveolar epithelial cells. *J. Immunol.* **168**, 1919–1925
24. Wetsel, R. A. (1995) Expression of the complement C5a anaphylatoxin receptor (C5aR) on non-myeloid cells. *Immunol. Lett.* **44**, 183–187
25. Drouin, S. M., Kildsgaard, J., Haviland, J., Zabner, J., Jia, H. P., McCray, P. B., Jr., Tack, B. F., and Wetsel, R. A. (2001) Expression of the complement anaphylatoxin C3a and C5a receptors on bronchial epithelial and smooth muscle cells in models of sepsis and asthma. *J. Immunol.* **166**, 2025–2032
26. Kwan, W. H., van der Touw, W., Paz-Artal, E., Li, M. O., and Heeger, P. S. (2013) Signaling through C5a receptor and C3a receptor diminishes function of murine natural regulatory T cells. *J. Exp. Med.* **210**, 257–268
27. Dunkelberger, J., Zhou, L., Miwa, T., and Song, W. C. (2012) C5aR expression in a novel GFP reporter gene knockin mouse: implications for the mechanism of action of C5aR signaling in T cell immunity. *J. Immunol.* **188**, 4032–4042
28. Cain, S. A., and Monk, P. N. (2002) The orphan receptor C5L2 has high affinity binding sites for complement fragments C5a and C5a des-Arg(74). *J. Biol. Chem.* **277**, 7165–7169
29. Okinaga, S., Slattery, D., Humbles, A., Zsengeller, Z., Morteau, O., Kinrade, M. B., Brodbeck, R. M., Krause, J. E., Choe, H. R., Gerard, N. P., and Gerard, C. (2003) C5L2, a nonsignaling C5A binding protein. *Biochemistry* **42**, 9406–9415
30. Chen, N. J., Mirtsos, C., Suh, D., Lu, Y. C., Lin, W. J., McKerlie, C., Lee, T., Baribault, H., Tian, H., and Yeh, W. C. (2007) C5L2 is critical for the biological activities of the anaphylatoxins C5a and C3a. *Nature* **446**, 203–207
31. Li, R., Coulthard, L. G., Wu, M. C., Taylor, S. M., and Woodruff, T. M. (2013) C5L2: a controversial receptor of complement anaphylatoxin, C5a. *FASEB J.* **27**, 855–864
32. Rittirsch, D., Flierl, M. A., Nadeau, B. A., Day, D. E., Huber-Lang, M., Mackay, C. R., Zetoune, F. S., Gerard, N. P., Cianflone, K., Kohl, J., Gerard, C., Sarma, J. V., and Ward, P. A. (2008) Functional roles for C5a receptors in sepsis. *Nat. Med.* **14**, 551–557

33. Zhang, X., Schmudde, I., Laumonnier, Y., Pandey, M. K., Clark, J. R., Konig, P., Gerard, N. P., Gerard, C., Wills-Karp, M., and Kohl, J. (2010) A critical role for C5L2 in the pathogenesis of experimental allergic asthma. *J. Immunol.* **185,** 6741–6752

34. Kohl, J., Baelder, R., Lewkowich, I. P., Pandey, M. K., Hawlisch, H., Wang, L., Best, J., Herman, N. S., Sproles, A. A., Zwirner, J., Whitsett, J. A., Gerard, C., Sfyroera, G., Lambris, J. D., and Wills-Karp, M. (2006) A regulatory role for the C5a anaphylatoxin in type 2 immunity in asthma. *J. Clin. Invest.* **116,** 783–796

35. Bosmann, M., Sarma, J. V., Atefi, G., Zetoune, F. S., and Ward, P. A. (2012) Evidence for anti-inflammatory effects of C5a on the innate IL-17A/IL-23 axis. *FASEB J.* **26,** 1640–1651

36. Hawlisch, H., Belkaid, Y., Baelder, R., Hildeman, D., Gerard, C., and Kohl, J. (2005) C5a negatively regulates toll-like receptor 4-induced immune responses. *Immunity* **22,** 415–426

37. Bosmann, M., Haggadone, M. D., Zetoune, F. S., Sarma, J. V., and Ward, P. A. (2013) The interaction between C5a and both C5aR and C5L2 receptors is required for production of G-CSF during acute inflammation. *Eur. J. Immunol.* **43,** 1907–1913

38. Brinkmann, V., Reichard, U., Goosmann, C., Fauler, B., Uhlemann, Y., Weiss, D. S., Weinrauch, Y., and Zychlinsky, A. (2004) Neutrophil extracellular traps kill bacteria. *Science* **303,** 1532–1535

39. Brinkmann, V., and Zychlinsky, A. (2007) Beneficial suicide: why neutrophils die to make NETs. *Nat. Rev. Microbiol.* **5,** 577–582

40. Hakkim, A., Fuchs, T. A., Martinez, N. E., Hess, S., Prinz, H., Zychlinsky, A., and Waldmann, H. (2011) Activation of the Raf-MEK-ERK pathway is required for neutrophil extracellular trap formation. *Nat. Chem. Biol.* **7,** 75–77

41. Li, P., Li, M., Lindberg, M. R., Kennett, M. J., Xiong, N., and Wang, Y. (2010) PAD4 is essential for antibacterial innate immunity mediated by neutrophil extracellular traps. *J. Exp. Med.* **207,** 1853–1862

42. Fuchs, T. A., Abed, U., Goosmann, C., Hurwitz, R., Schulze, I., Wahn, V., Weinrauch, Y., Brinkmann, V., and Zychlinsky, A. (2007) Novel cell death program leads to neutrophil extracellular traps. *J. Cell Biol.* **176,** 231–241

43. Clark, S. R., Ma, A. C., Tavener, S. A., McDonald, B., Goodarzi, Z., Kelly, M. M., Patel, K. D., Chakrabarti, S., McAvoy, E., Sinclair, G. D., Keys, E. M., Allen-Vercoe, E., Devinney, R., Doig, C. J., Green, F. H., and Kubes, P. (2007) Platelet TLR4 activates neutrophil extracellular traps to ensnare bacteria in septic blood. *Nat. Med.* **13,** 463–469

44. Fuchs, T. A., Brill, A., Duerschmied, D., Schatzberg, D., Monestier, M., Myers, D. D., Jr., Wrobleski, S. K., Wakefield, T. W., Hartwig, J. H., and Wagner, D. D. (2010) Extracellular DNA traps promote thrombosis. *Proc. Natl. Acad. Sci. U. S. A.* **107,** 15880–15885

45. Gerard, N. P., Lu, B., Liu, P., Craig, S., Fujiwara, Y., Okinaga, S., and Gerard, C. (2005) An anti-inflammatory function for the complement anaphylatoxin C5a-binding protein, C5L2. *J. Biol. Chem.* **280,** 39677–39680

46. Bernard, G. R., Artigas, A., Brigham, K. L., Carlet, J., Falke, K., Hudson, L., Lamy, M., Legall, J. R., Morris, A., and Spragg, R. (1994) The American-European Consensus Conference on ARDS. Definitions, mechanisms, relevant outcomes, and clinical trial coordination. *Am. J. Resp. Crit. Care Med.* **149,** 818–824

47. Paine, R., 3rd, Standiford, T. J., Dechert, R. E., Moss, M., Martin, G. S., Rosenberg, A. L., Thannickal, V. J., Burnham, E. L., Brown, M. B., and Hyzy, R. C. (2012) A randomized trial of recombinant human granulocyte-macrophage colony stimulating factor for patients with acute lung injury. *Crit. Care Med.* **40,** 90–97

48 Bosmann, M., Grailer, J. J., Zhu, K., Matthay, M. A., Sarma, J. V., Zetoune, F. S., and Ward, P. A. (2012) Anti-inflammatory effects of beta2 adrenergic receptor agonists in experimental acute lung injury. *FASEB J.*

49. Monestier, M., Fasy, T. M., Losman, M. J., Novick, K. E., and Muller, S. (1993) Structure and binding properties of monoclonal antibodies to core histones from autoimmune mice. *Mol. Immunol.* **30,** 1069–1075

50. Xu, J., Zhang, X., Pelayo, R., Monestier, M., Ammollo, C. T., Semeraro, F., Taylor, F. B., Esmon, N. L., Lupu, F., and Esmon, C. T. (2009) Extracellular histones are major mediators of death in sepsis. *Nat. Med.* **15,** 1318–1321

51. Larsen, G. L., McCarthy, K., Webster, R. O., Henson, J., and Henson, P. M. (1980) A differential effect of C5a and C5a des Arg in the induction of pulmonary inflammation. *Am. J. Pathol.* **100,** 179–192

52. Karsten, C. M., Pandey, M. K., Figge, J., Kilchenstein, R., Taylor, P. R., Rosas, M., McDonald, J. U., Orr, S. J., Berger, M., Petzold, D., Blanchard, V., Winkler, A., Hess, C., Reid, D. M., Majoul, I. V., Strait, R. T., Harris, N. L., Kohl, G., Wex, E., Ludwig, R., Zillikens, D., Nimmerjahn, F., Finkelman, F. D., Brown, G. D., Ehlers, M., and Kohl, J. (2012) Anti-inflammatory activity of IgG1 mediated by Fc galactosylation and association of FcgammaRIIB and dectin-1. *Nat. Med.* **18,** 1401–1406

53. Bamberg, C. E., Mackay, C. R., Lee, H., Zahra, D., Jackson, J., Lim, Y. S., Whitfeld, P. L., Craig, S., Corsini, E., Lu, B., Gerard, C., and Gerard, N. P. (2010) The C5a receptor (C5aR) C5L2 is a modulator of C5aR-mediated signal transduction. *J. Biol. Chem.* **285,** 7633–7644

54. Garcia, C. C., Weston-Davies, W., Russo, R. C., Tavares, L. P., Rachid, M. A., Alves-Filho, J. C., Machado, A. V., Ryffel, B., Nunn, M. A., and Teixeira, M. M. (2013) Complement C5 activation during influenza A infection in mice contributes to neutrophil recruitment and lung injury. *PloS One* **8,** e64443

55. Kanse, S. M., Gallenmueller, A., Zeerleder, S., Stephan, F., Rannou, O., Denk, S., Etscheid, M., Lochnit, G., Krueger, M., and Huber-Lang, M. (2012) Factor VII-activating protease is activated in multiple trauma patients and generates anaphylatoxin C5a. *J. Immunol.* **188,** 2858–2865

56. Bosch, X., Poch, E., and Grau, J. M. (2009) Rhabdomyolysis and acute kidney injury. *N. Engl. J. Med.* **361,** 62–72

57. Zhang, Q., Raoof, M., Chen, Y., Sumi, Y., Sursal, T., Junger, W., Brohi, K., Itagaki, K., and Hauser, C. J. (2010) Circulating mitochondrial DAMPs cause inflammatory responses to injury. *Nature* **464,** 104–107

58. Abrams, S. T., Zhang, N., Manson, J., Liu, T., Dart, C., Baluwa, F., Wang, S. S., Brohi, K., Kipar, A., Yu, W., Wang, G., and Toh, C. H. (2013) Circulating histones are mediators of trauma-associated lung injury. *Am. J. Respir. Crit. Care Med.* **187,** 160–169

59. Hirsch, J. G. (1958) Bactericidal action of histone. *J. Exp. Med.* **108,** 925–944

60. Lee, D. Y., Huang, C. M., Nakatsuji, T., Thiboutot, D., Kang, S. A., Monestier, M., and Gallo, R. L. (2009) Histone H4 is a major component of the antimicrobial action of human sebocytes. *J. Invest. Dermatol.* **129,** 2489–2496

61. Allam, R., Scherbaum, C. R., Darisipudi, M. N., Mulay, S. R., Hagele, H., Lichtnekert, J., Hagemann, J. H., Rupanagudi, K. V., Ryu, M., Schwarzenberger, C., Hohenstein, B., Hugo, C., Uhl, B., Reichel, C. A., Krombach, F., Monestier, M., Liapis, H., Moreth, K., Schaefer, L., and Anders, H. J. (2012) Histones from dying renal cells aggravate kidney injury via TLR2 and TLR4. *J. Am. Soc. Nephrol.* **23,** 1375–1388

62. Friggeri, A., Banerjee, S., Xie, N., Cui, H., De Freitas, A., Zerfaoui, M., Dupont, H., Abraham, E., and Liu, G. (2012) Extracellular histones inhibit efferocytosis. *Mol. Med.* **18,** 825–833

63. Caudrillier, A., Kessenbrock, K., Gilliss, B. M., Nguyen, J. X., Marques, M. B., Monestier, M., Toy, P., Werb, Z., and Looney, M. R. (2012) Platelets induce neutrophil extracellular traps in transfusion-related acute lung injury. *J. Clin. Invest.* **122,** 2661–2671

64. Saffarzadeh, M., Juenemann, C., Queisser, M. A., Lochnit, G., Barreto, G., Galuska, S. P., Lohmeyer, J., and Preissner, K. T. (2012) Neutrophil extracellular traps directly induce epithelial and endothelial cell death: a predominant role of histones. *PloS One* **7,** e32366

65. Xu, J., Zhang, X., Monestier, M., Esmon, N. L., and Esmon, C. T. (2011) Extracellular histones are mediators of death through TLR2 and TLR4 in mouse fatal liver injury. *J. Immunol.* **187,** 2626–2631

66. Gotts, J. E., and Matthay, M. A. (2011) Mesenchymal stem cells and acute lung injury. *Crit. Care Clin.* **27,** 719–733